

# Stationary State Skewness in Two Dimensional KPZ Type Growth.

Chen-Shan Chin and Marcel den Nijs

*Department of Physics, University of Washington, P.O. Box 351560,  
Seattle, Washington 98195-1560*

We present numerical Monte Carlo results for the stationary state properties of KPZ type growth in two dimensional surfaces, by evaluating the finite size scaling (FSS) behaviour of the 2nd and 4th moments,  $W_2$  and  $W_4$ , and the skewness,  $W_3$ , in the Kim-Kosterlitz (KK) and BCSOS model. Our results agree with the stationary state proposed by Lässig. The roughness exponents  $W_n \sim L^{\alpha_n}$  obey power counting,  $\alpha_n = n\alpha$ , and the amplitude ratio's of the moments are universal. They have the same values in both models:  $W_3/W_2^{1.5} = -0.27$  (1) and  $W_4/W_2^2 = +3.15$  (2). Unlike in one dimension, the stationary state skewness is not tunable, but a universal property of the stationary state distribution. The FSS corrections to scaling in the KK model are weak and  $\alpha$  converges well to the Kim-Kosterlitz-Lässig value  $\alpha = \frac{2}{5}$ . The FSS corrections to scaling in the BCSOS model are strong. Naive extrapolations yield a smaller value,  $\alpha \simeq 0.38(1)$ , but are still consistent with  $\alpha = \frac{2}{5}$  if the leading irrelevant corrections to FSS scaling exponent is of order  $y_{ir} \simeq -0.6$  (2).

PACS numbers: 02.50.Ey, 05.40+j, 68.35.Fx

## I. INTRODUCTION

KPZ type growth is one of the generic dynamic processes describing growth of crystal surfaces. It is named after the Langevin equation introduced by Kardar, Parisi, and Zhang about a decade ago [1–5].

$$\frac{\partial h}{\partial t} = \nu \frac{\partial h^2}{\partial x^2} + \lambda \left( \frac{\partial h}{\partial x} \right)^2 + \eta \quad (1)$$

with  $\eta$  uncorrelated noise

$$\langle \eta(x_1, t_1) \eta(x_2, t_2) \rangle = D \delta(t_1 - t_2) \delta(x_1 - x_2) \quad (2)$$

Numerous microscopic models on the master equation level have been studied numerically as well and are confirmed to be in the KPZ universality class [2–5]. However, many properties of this process are still in question, including basic aspects, like the precise values of the scaling critical exponents, and the detailed structure of the stationary growing state. Part of the problem is the absence of an obvious mean field theory. The linear, integrable diffusion, part of the KPZ equation ( $\lambda = 0$ ) does not play the role of mean field theory fixed point in high enough dimensions ( $D$ ). The KPZ behaviour is governed by a strong coupling fixed point for all  $D$ , and thus evades perturbative renormalization treatments [6].

It is widely accepted that the dynamic exponent  $z$  and the stationary state roughness exponent  $\alpha$  obey the equality  $\alpha + z = 2$  in all  $D$  [2–5]. These critical exponents specify how time and height rescale under a renormalization transformation:  $x \rightarrow bx$ ,  $t \rightarrow b^z t$ , and  $h \rightarrow b^\alpha h$ . The exponent identity states that under renormalization the amplitude of the non-linear term in the KPZ equation does not change.  $\lambda$  is a so-called redundant scaling field. It plays a role similar to lattice anisotropy in equilibrium phase transitions. Increasing  $\lambda$  simply speeds-up the process, and scaling amplitudes are proportional to  $\lambda$ .

This exponent equality links the dynamic scaling to the stationary state scaling. Therefore the focus has shifted recently to the structure of the stationary state.

The stationary growing state is trivial in one dimension ( $1D$ ). It is the Gaussian distribution. The up and down steps along the surface are uncorrelated beyond a definite correlation length. This implies  $\alpha = \frac{1}{2}$  (the random walk value), and from the above exponent identity it follows that  $z = \frac{3}{2}$ . This behaviour is well established, not only by numerical studies [2–5], but also analytically. The  $1D$  body centered solid on solid (BCSOS) growth model is exactly soluble [7,8]. Its master equation is a special case of the  $2D$  equilibrium 6-vertex model. In the latter representation, KPZ scaling describes facet ridge end-points of equilibrium crystal shapes [9].  $1D$  KPZ growth is equivalent also to asymmetric exclusion hopping processes [10]. Moreover, the exact stationary state of the Langevin equation itself is known in  $1D$  and is indeed the Gaussian distribution [5].

The stationary state is not simple in  $D > 1$ . The stationary state roughness exponent  $\alpha$  takes a non-trivial value and is actually not very well known numerically. For example, in  $2D$  the reported values vary between  $\alpha = 0.37 - 0.4$  [3,4,11–13]. Lässig made an important analytical break through last year [14]. He proposed the likely structure of the stationary state by studying the operator product expansion of the (height variable) correlation functions. Under the assumption that the algebra closes and contains only one scaling field operator, Lässig obtained a quantization condition for the exponents. One of these solutions,  $\alpha = \frac{2}{5}$ , is close to the above  $2D$  numerical values. The moments

$$W_n = \langle (h_i - \bar{h})^n \rangle \quad (3)$$

of Lässig's stationary state distribution obey power counting, i.e., the exponents in the scaling relations

$$W_n(N^{-1}, t^{-1}) = b^{\alpha n} W_n(bN^{-1}, b^z t^{-1}). \quad (4)$$

are related as  $\alpha_n = n\alpha$ . The distribution lacks multi scaling. Moreover, for the closure of the algebra it is important that the stationary state is skewed. The odd moments, in particular the third one must be non-zero.

In this paper we report a detailed numerical study of the stationary state in 2D for the Kim-Kosterlitz (KK) [11] and the BCSOS model. We determine the finite size scaling behaviour of the second, third, and fourth moments.

In section 2 we review the properties of stationary state skewness in 1D KPZ growth, and list the possibilities in higher dimensions. Section 3 contains our numerical results for the KK and BCSOS model. The third moment is indeed non-zero and the second, third, and fourth moments obey indeed power counting. We find strong evidence that the amplitude ratio's of the moments are universal,  $R_3 = W_3/W_2^{1.5} = -0.27(1)$  and  $R_4 = W_4/W_2^2 = +3.15(2)$ . The amount of stationary state skewness is the same in these two models. In 1D skewness is tunable, but appears not to be so in 2D. The values of these amplitude ratio's are the major new results of this paper.

In section 3 we address also whether the difference in the previously reported values of  $\alpha$  for the KK and BCSOS models can be attributed to finite size scaling (FSS) type corrections. The FSS corrections to scaling exponent is large, but in the same range of values suggested by naive power counting.

To check more directly whether skewness is tunable or not, we introduce a temperature type parameter  $K$  in the BCSOS model. In the KK model it is known that  $\lambda$  changes sign with  $K$  [12]. In section 4 we give an intuitive explanation for why this happens. (It is related to pre-roughening phenomena in equilibrium surfaces.) In the BCSOS model  $\lambda$  does not change sign. In section 5 we present MC data for the  $K$  dependence of the roughness exponents and the amplitude ratio's. Both show some systematic drift, but much smaller than expected if they would vary with  $K$ .

## II. STATIONARY STATE SKEWNESS

This study was actually not motivated by Lässig's recent results. It was conceived as a generalization of an earlier study of stationary state skewness in 1D [15]. The KK model is a special point in the restricted solid-on-solid (RSOS) model. We varied its adsorption and evaporation probabilities in the 1D model by making them dependent on the local nearest neighbour heights. That lead to 5 independent parameters. Surprisingly we were able to construct the exact stationary state in a 4 dimensional subspace. Its structure is simple. The steps in the interface are completely uncorrelated. Only the step density varies. This state has zero skewness. It is a Gaussian and has particle-hole symmetry. Outside this exact soluble subspace the stationary state is skewed. This means

that in general KPZ type growth in 1D has a non-zero third moment  $W_3$  in its stationary state. For example, the KK point lies outside the non-skewed subspace. On the other hand, the stationary states in the exactly soluble BCSOS model and also the Langevin equation itself are non-skewed. Stationary state skewness is distinct from temporal skewness. Most initial states develop into skewed structures at intermediate time scales (temporal skewness) even if the stationary state is not skewed [16].

So in 1D, KPZ type stationary states are typically skewed, and its amplitude is tunable. This raises the immediate question whether skewness affects the scaling exponents. Let's refer to the operators leading out of the non-skewed subspace as  $\mathcal{O}_{sk}$  and to their conjugate coupling constants as  $u_{sk}$ . In 1D, a KPZ type fixed point with zero-skewness exists. The question is whether this fixed point is stable; whether  $\mathcal{O}_{sk}$  is a relevant, marginal, redundant, or an irrelevant operator. Suppose the non-skewed KPZ fixed point is stable. The moments should scale then with system size as

$$W_n(N^{-1}, u_{sk}) = b^{\alpha_n} W_n(bN^{-1}, b^{y_{sk}} u_{sk}) \quad (5)$$

with  $\alpha_n = n\alpha$  and  $y_{sk} < 0$ . All even moments scale as

$$W_n \simeq AN^{\alpha_n} + \dots \quad (6)$$

with universal amplitude ratio's,  $R_n = W_n/W_2^{n/2}$ . All odd moments scale as

$$\begin{aligned} W_n(N^{-1}, u_{sk}) &= N^{\alpha_n} \mathcal{F}_n(N^{y_{sk}} u_{sk}) \\ &= N^{\alpha_n} [\mathcal{F}_n(0) + \mathcal{F}'_n(0) N^{y_{sk}} u_{sk} + \dots] \\ &\sim u_{sk} N^{\alpha_n + y_{sk}} \end{aligned} \quad (7)$$

with  $\mathcal{F}_n(0) = 0$  because the fixed point has no skewness. The odd amplitude ratio's are proportional to  $u_{sk}$ , i.e., the skewness varies continuously.

Numerical (transfer matrix finite size scaling) results confirmed that the non-skewed KPZ fixed point is stable in 1D. We found  $y_{sk} \simeq -1$ . Moreover, the amplitude of  $W_3$  (at e.g., the KK point) is indeed roughly proportional to the skewness coupling constant  $u_{sk}$ , in accordance with eq.7.

Skewness is negative at the 1D KK point. On average hill tops are wider (flatter, less sharp) than valley bottoms. Such a statement is meaningless without a specification of a cut-off. The definition of what constitutes a mountain and what represents a local hump depends on the length scale at which the surface configuration is being viewed. (Humans do not interpret every grain of sand as a hill.) Skewness is a scale dependent property. The asymptotic scaling of the moments tells us how asymmetric the hills and valleys are in the large length scale limit. In 1D this skewness persists all the way to microscopic length scales. We calculated the surplus of sharp valley bottoms over sharp hill tops at the microscopic (the grains of sand) level. This expectation value has the same sign as the macroscopic skewness and is also roughly proportional to  $u_{sk}$ . This invariance of the

surface structure over all length scales is related to the rather trivial nature of the fixed point stationary state (Gaussian distribution).

The tunability of the skewness at the microscopic length scale is easy to understand. Consider the 1D RSOS model with deposition only, with three parameters:  $p_h$ ,  $p_s$ , and  $p_v$  [15]. The density of local sharp hill tops is set by the deposition probability  $p_h$  of particles on local flat surface segments. The sharpness of these local hilltops is set by the rate at which they broaden, i.e., the probability with which particles adhere to existing steps,  $p_s$ . The density of local sharp valleys is set by the rate at which single particle puddles fill-up,  $p_v$  compared to the rate at which they are created,  $2p_s$ . These processes balance exactly inside the subspace where the stationary state is trivial and has zero skewness. At the KK point,  $p_h = p_s = p_v = 1$ , the balance is imperfect and the dynamics creates a backlog of “to-be-filled-up” local valleys. Newly created local hill tops broaden readily, and therefore are flatter [15].

Is the skewness tunable in  $D > 1$  as well? Is there maybe a line of KPZ type fixed points with continuously varying skewness? A varying exponent  $\alpha$  would explain the current numerical spread in its value. Is it possible to change the sign of skewness without changing the sign of  $\lambda$  in eq.(1)? Or, is there one single KPZ stationary state fixed point distribution, with a universal amount (and sign) of skewness? In that case we need to explain the numerical spread in  $\alpha$ 's in terms of strong FSS corrections. These are the issues we address in this paper.

### III. SCALING OF THE STATIONARY STATE MOMENTS

We perform a systematic numerical study of the stationary state properties in the 2D KK-model and the BCSOS model. In both cases we allow only particle deposition (no desorption). Consider a 2D square lattice with an height variable  $h(r) = 0, \pm 1, \pm 2, \dots$  at each lattice site. We apply periodic boundary conditions. In the KK-model, nearest neighbour columns are allowed to differ by at most one unit,  $\delta h = 0, \pm 1$ . Choose a site at random, and deposit a particle,  $h \rightarrow h + 1$ , with probability  $p = 1$  unless such a move would violate the above restriction.

In the BCSOS model the square lattice is divided into two sublattices. The height variables are restricted to be even on one of them,  $h(r) = 0, \pm 2, \dots$ , and to be odd on the other  $h(r) = \pm 1, \pm 3, \dots$ , such that nearest neighbour columns always differ in height by one  $\delta h = \pm 1$ . Choose at random a site, and deposit a particle with probability  $p = 1$  if the move does not violate the  $\delta h = \pm 1$  constraint. In section V we consider also the generalization where the BCSOS deposition probabilities vary with the local configuration by means of a temperature type parameter,  $p = \min(1, \exp(-\Delta E))$ .  $\Delta E$  is the energy change if the adsorption would take place. The energy

$$E(\{h_i\}) = \sum_{\langle i,j \rangle} \frac{1}{4} K (h_i - h_j)^2 \quad (8)$$

has a tunable parameter  $K$  and the summation runs over all next nearest neighbours. This rule is identical to that in standard Metropolis MC simulations, except that desorption is forbidden. The latter breaks detailed balance and leads to the non-equilibrium growing stationary state.

We determine the second, third, and fourth moments of the stationary states. The MC averages in this section involve  $\simeq 2 \cdot 10^6$  MC steps, after  $\simeq 4 \cdot 10^3$  initial MC configurations, to allow the surface to reach its stationary state. The square lattice size  $L^2$  varies between  $12 \leq L \leq 128$ .

First consider the KK model. Fig. 1 shows the second moment  $W_2$ . It scales as  $W_2 \simeq AL^{\alpha_2}$ . The slope of the log-log plot gives the exponent  $\alpha_2$ . It is a mistake to apply a least-square type fit to the slope at large  $L$ . One should determine the slope at various system size intervals and perform a finite size scaling (FSS) analysis. Fig. 2 represents such an analysis. It shows FSS estimates for  $\alpha_2$  from the same data, defined as  $\alpha_2(L) = \log[W_2(L_2)/W_2(L_1)]/\log[L_2/L_1]$  with  $L_2 \simeq 1.2L_1$  and  $L = \frac{1}{2}(L_1 + L_2)$ . Such a FSS scaling analysis is only barely feasible at large system sizes due to the intrinsic MC noise. Fig. 2 is indeed rather noisy at large  $L$ . The MC scatter increases with system size, since the stationary state is intrinsically critical and therefore subject to critical slowing down. We opted for running many lattice sizes instead of fewer but longer MC runs. The solid line is obtained by averaging the  $\alpha_2(L)$  locally, over  $L - 7 \leq L \leq L + 7$ . The data in Fig. 2 converge by eye to  $\alpha_2 = 0.80(2)$ , consistent with the value  $\alpha = \frac{2}{5}$  proposed by Kim and Kosterlitz from their earlier numerical results [11,12], and with Lässig's [14] stationary state. The FSS corrections to scaling in the KK model are small compared to the MC noise.

Figs. 3 and 4 show the same FSS analysis for the third and fourth moment exponents  $\alpha_3$  and  $\alpha_4$ . They converge by eye to  $\alpha_3 = 1.20(4)$  and  $\alpha_4 = 1.60(5)$ . This agrees with Lässig's stationary state. In particular, the surface is skewed, and power counting,  $\alpha_n = n\alpha$ , is satisfied within the numerical accuracy. The corrections to FSS are again small compared to the MC noise.

Figs. 5 and 6 show the amplitude ratio's (the circles) of the third and fourth moment compared to the second one,  $R_n = W_n/(W_2)^{n/2}$ . The fact that these ratio's convergence gives additional evidence of the validity of power counting. Actually, they do so much smoother than the exponents  $\alpha_n$ , suggesting that the MC fluctuations tend to preserve the power counting property better than the precise value of  $\alpha$ . The amplitude ratio's converge smoothly to  $R_3 = -0.27(1)$  and  $R_4 = +3.15(2)$ . Skewness is negative,  $R_3 < 0$ . It is probably wishful thinking to guess that  $R_4 = \pi$ . ( $R_4 = 3$  in Gaussian distributions.)

Consider the BCSOS model at  $K = 0$ . Figs. 7, 8, and 9 show the same type of FSS estimates for the exponents  $\alpha_n$ . The finite size corrections to scaling are much larger than in the KK model. The data converge by eye systematically to smaller values than in the KK model:  $\alpha_2 = 0.77(2)$ ,  $\alpha_3 = 1.16(3)$ , and  $\alpha_4 = 1.54(4)$ . This is consistent with the value for  $\alpha_2$  reported in the literature [4,13]. These  $\alpha_n$ 's are mutually consistent with power counting. Power counting is again more stable than the values of the exponents  $\alpha_n$ . Most importantly, the amplitude ratio's in Figs. 5 and 6 (the diamonds) converge to the same values as in the KK model (the circles).

Is  $\alpha$  really smaller than in the KK model and different from the Kim-Kosterlitz-Lässig (KKL) value? The finite size scaling corrections in the BCSOS model are several orders of magnitude bigger than in the KK model. Is it believable that these apparent differences are due to corrections to scaling only? The above FSS extrapolation "by eye" presumes implicitly that all  $\alpha_n$  converge approximately linearly in  $L^{-1}$ . This looks reasonable from the data, but is too restrictive. Corrections to scaling originate from so-called irrelevant scaling fields. The corrections to scaling exponents  $y_{ir} < 0$  in  $W_n \simeq A_n N^{\alpha_n} [1 + B_n L^{y_{ir}} + \dots]$  are universal properties of the stationary state fixed point. The amplitudes  $B_n$  are not universal. They depend on the "distance" of the model to the fixed point and the quantity we are looking at. Assume that one correction to scaling term dominates, i.e., that all other operators scale with much more negative values of  $y_{ir}$ . The same exponent  $y_{ir}$  should then appear in all moments. The only exception is that in specific quantities the leading term might have zero amplitude by symmetry. For example, all even moments might show a different leading exponent  $y_{ir}$  than all odd ones. This actually happens here.

Suppose we force our BCSOS data to converge to  $\alpha = \frac{2}{5}$ . We made plots of  $W_n/L^{n\alpha}$  with  $\alpha = \frac{2}{5}$  versus  $L^{y_{ir}}$  for a range of values of  $y_{ir}$ . This should be a straight line at the proper  $y_{ir}$ . From this we estimate that  $y_{ir} \simeq -0.6$  (2) for the second and fourth moments, and  $y_{ir} \simeq -1.7$  (3) for the third moment. These straight line fits are satisfactory stable. So the KKL value for  $\alpha$  is within the realm of possibilities for the BCSOS model. Still, it remains a leap of faith, because the curves in Figs. 7, 8, and 9, are bend to the limit.

It would be much more convincing if the corrections to scaling exponents where known analytically, and/or take simple values. At the core of Lässig's result is the assumption that the operator content of the system is simply. Therefore one would expect that the irrelevant operators have rather trivial critical dimensions, like integers, multiples of  $\alpha$ , and combinations of both. The above numerical values of  $y_{ir}$  do not look that simple, but are of the same order of magnitude as we might expect. Simple minded power counting in Eq.(1) with  $\alpha = \frac{2}{5}$  and  $z + \alpha = 2$ , suggests that the corrections to scaling are strong; that the curvature operator  $\partial^2 h / \partial x^2$  is irrel-

evant, but not by much,  $y_\nu = -\alpha$ , and that the leading skewness operator  $(\partial^2 h / \partial x^2)^2$  scales with  $y_{sk} = -2$ .

#### IV. TEMPERATURE DEPENDENT TRANSITION PROBABILITIES

In section V we vary the temperature type parameter  $K$  in the BCSOS model, to study the universality of  $\alpha$  and skewness issues raised in section III in more detail. We do this only for the BCSOS model, not the RSOS model. (The KK model is a special point in the latter.) From earlier studies it is known that in the RSOS model the KPZ non-linear term  $\lambda$  changes sign with  $K$  [12]. This creates strong Edwards-Wilkinson (EW) type corrections to scaling and will obscure the skewness property, because the EW stationary state at  $\lambda = 0$  is non-skewed (the Gaussian distribution). Such a change in  $\lambda$  does not take place in the BCSOS model.

The following connection with preroughening phenomena in equilibrium crystal surface explains why  $\lambda$  changes sign in the RSOS model and not in the BCSOS model. Imagine a two dimensional phase diagram, with  $K \sim T^{-1}$  the temperature like parameter, and a parameter  $s$  representing the asymmetry between particle deposition and evaporation.  $s = 0$  corresponds to MC equilibrium type dynamics and  $s = 1$  to the above pure deposition model without evaporation. The equilibrium surface undergoes a roughening transition. The rough phase is the EW stationary state. The scaling properties of the equilibrium (stationary) state are described by the Gibbs distribution of the sine-Gordon model

$$E = \int dx dy \left[ \frac{K}{2} (\nabla h)^2 + u_2 \cos(2\pi h) + u_4 \cos(4\pi h) \right] \quad (9)$$

It is known that  $u_2$  varies with temperature and changes sign inside the equilibrium rough phase in the RSOS model just above the roughening transition. This follows from an exact duality transformation [17]. The location of this  $u_2 = 0$  point at  $s = 0$  agrees qualitatively with the numerical value of the  $\lambda = 0$  point at  $s = 1$ . Those values do not have to be identical. They only need to be of the same order of magnitude. The following arguments suggest that a line of  $\lambda = 0$  points emerges from the  $u_2 = 0$  point at  $s = 0$  into the  $s$  direction.

$u_2$  is negative at the high temperature side of the  $u_2 = 0$  line. There, the rough stationary state surface takes locally the so-called disordered flat type structure with alternating up and down steps and local half integer surface height [18]. This is the same surface structure as in the BCSOS model (but not close-packed with  $dh = \pm 1$  kinks). The non-linear term in the KPZ equation controls the local growth velocity at sloped sections of the surface. Growth at slopes is suppressed in BCSOS type rough structures, and therefore  $\lambda < 0$ . At the opposite,

low temperature  $u_2 > 0$  side of the  $u_2 = 0$  point, the local rough RSOS surface is smooth, and has on the local level integer average surface heights. In such structures, growth at sloped parts of the surface is enhanced and therefore  $\lambda > 0$ .

The location of  $u_2 = 0$  can be controlled by introducing further neighbour interactions. This point transforms into the preroughening transition point when it moves below the roughening temperature [18]. (But only at  $s \neq 0$ , because the driven non-equilibrium surface is always rough).

Such a change in  $\lambda$  does not take place in the BC-SOS model. Its equilibrium stationary state (at  $s = 0$ ) is exactly known for all  $K$  from the exact solution of the 6-vertex model [19].  $u_2$  is negative at all values of  $K$  in the  $s = 0$  equilibrium surface. Therefore there is no reason to expect a change of  $\lambda$  as function of  $K$  in the pure deposition model at  $s = 1$ . This makes the BCSOS model a suitable testing ground for the tunability of 2D skewness and the universality of  $\alpha$ .

## V. TEMPERATURE DEPENDENT DEPOSITION RATES IN THE BCSOS MODEL

In this section we study the universality of the stationary state roughness exponent  $\alpha$  and the skewness by varying the deposition probabilities in the BCSOS model. This should clarify whether the skewness is truly universal or a tunable parameter. We can control the microscopic particle-hole asymmetry explicitly.

Fig. 10 shows the variation of the second moment exponent  $\alpha_2(L)$  with the temperature parameter  $K$ . This plot is more qualitative than the ones in section III. The system sizes are smaller (up to  $L=80$ ) and the MC runs an order of magnitude shorter (up to  $10^5$  MC steps, after 2500 initial MC steps). The curves have a definite slope at small system sizes, but these disappear with system size. At temperatures beyond  $K \simeq 1$  the surface becomes very flat and inactive. Compared to  $K \simeq 0$  the system size is effectively much smaller and the MC runs effectively much shorter. This explains the decay in the approximants at large  $K$ . At the opposite side, beyond  $K \simeq -1$ , the surface becomes quite faceted at short distances and the dynamics slows down again. Faceted structures have  $\alpha = 1$ . This explains why the  $\alpha_2(L)$  curves drift upward on the left hand side in Fig. 10.  $\alpha_3$  and  $\alpha_4$  vary also only weakly with  $K$ . The amplitude ratios  $R_3 = W_3/W_2^{1.5}$  and  $R_4 = W_4/W_2^2$  do not vary significantly with  $K$  either.

We performed quantitative MC runs at  $K = \pm 0.25, \pm 0.1$  for system sizes up to  $L = 60$  (with  $2 \cdot 10^6$  MC step runs after  $4 \cdot 10^3$  initial MC steps). Figs. 11, 12, and 13 show the  $\alpha_n(L)$  approximants as function of  $1/L$  at  $K = \pm 0.25$ . The  $K = 0$  data is included as reference. The corrections to scaling in the even moments increase with  $K$ , and are an order of magnitude smaller

at  $K = -0.25$ . The three curves are consistent with convergence towards the same values for  $\alpha_2$  and  $\alpha_4$ . Naively these values point to an  $\alpha$  smaller than  $\frac{2}{5}$ , but still consistent with the KKL value if the crossover scaling exponent is large (see section III). The corrections to scaling in  $\alpha_3$  are less clear cut. At first glance the three curves seem more or less parallel (which would suggest a continuous variation in  $\alpha_3$  with  $K$ ), but they actually converge to indistinguishable values for  $\alpha_3$  given the error bar from the numerical MC noise.

The amplitude ratio's  $R_3 = W_3/W_2^{3/2}$  and  $R_4 = W_4/W_2^2$  are shown in Figs. 14 and 15. Like before these amplitude ratio's are more stable than the numerical values of  $\alpha_n$ . The data confirm universal  $K$ -independent values of  $R_n$  (although  $R_4$  drifts off by a few percent at  $K = 0.25$ ).

In 1D the skewness amplitude is tunable and directly related to the amount of particle-hole symmetry breaking at the microscopic level. Figs. 16 and 17 show how the microscopic particle-hole asymmetry varies as function of  $K$  in the 2D BCSOS model. We measure several local quantities. Fig. 16 shows the density difference ratio,  $\rho = (\rho_h - \rho_v)/(\rho_h + \rho_v)$ , between local sharp hill tops,  $\rho_h$ , and local sharp valleys,  $\rho_v$ , as seen along 1D cross-sections of the crystal. Fig. 17 shows the density difference  $\rho_{hv}$  between local sharp hill tops and local sharp valleys bottoms in the 2D surface and also the difference between sharp ridges versus sharp canyons  $\rho_{rc}$  as defined in Fig. 18. All three quantities vary dramatically with  $K$ . This demonstrates that the local skewness coupling constant  $u_{sk}$  varies significantly with  $K$ . Sufficiently to expect a large variation in  $R_3$  if (macroscopic) skewness is tunable. Since this not the case,  $R_3 \simeq -0.27$  is most likely a universal property of the stationary state.

The curves in Fig. 16 and Fig. 17 have kinks at  $K = 0$ . These are caused by the definition of the deposition probabilities,  $p = \min(1, \exp(-\Delta E))$ . The probabilities are temperature dependent for some configurations but constant,  $p = 1$ , for others. At  $K = 0$  they are being reshuffled. The curves of Fig. 10 have similar dips at  $K = 0$  for small  $L$ , but these vanish with system size. This is another illustration of the insensitivity of the macroscopic length scale properties of the stationary state on the local properties.

## VI. CONCLUSIONS

The most important result of this paper is that the amplitude ratio's  $R_3 = W_3/W_2^{1.5}$  and  $R_4 = W_4/W_2^2$  of the stationary state moments converge to the same value in the KK and BCSOS model,  $R_3 = -0.27(1)$  and  $R_4 = +3.15(2)$ . At the start of this project we expected that the skewness,  $R_3$ , would be the most sensitive parameter to test the universality of the KPZ stationary state properties in 2D. However,  $R_3$  is numerically much more stable than the surface roughness critical exponent

$\alpha$ .  $R_3$  takes the same value in the KK and BCSOS models, and does not vary significantly in the BCSOS model with the temperature parameter  $K$ ; in contrast to the strong variation in the microscopic measures of particle-hole asymmetry. The 2D KPZ stationary state skewness is universal, unlike 1D where it is tunable.

The differences in the numerical values for  $\alpha$  in the KK and BCSOS model have been a puzzle for a long time. The corrections to FSS scaling in the KK model are small, compared to the MC noise and point clearly to the KKL value  $\alpha = \frac{2}{5}$ . The FSS corrections to scaling in the BCSOS model are large. The stationary state roughness exponent converges naively but systematically to a smaller value  $\alpha \simeq 0.38$ . However, our FSS analysis shows that the data is consistent with  $\alpha = \frac{2}{5}$  if the leading corrections to scaling exponents are dominated by  $y_{ir} \simeq -0.6$  (2) for the even moments and  $y_{ir} \simeq -1.7$  (3) for the odd ones. These values are different, but in the same range as predicted by simple minded power counting. This is an important issue, because different values of  $\alpha$  in the KK and BCSOS models, and variations with  $K$  in the latter, would imply non-universality of 2D KPZ scaling, and open up the possibility of e.g., a continuously varying  $\alpha$ . Our data suggest one single KPZ fixed point with unique exponents. It is most likely Lässig's stationary state.

This work is supported by NSF grant DMR-9700430.

2332 (1990); J. Kim, T. Ala-Nissila, and J.M.Kosterlitz, Phys. Rev. Lett. **64**, 2333 (1990).

- [13] For numerical results on the 2D BCSOS model see e.g.: D. Liu and M. Plischke, Phys. Rev. B **38**, 4781 (1988); M. Koita and A.C. Levi, J.Phys.A **25**, 3121 (1992); B.M. Forrest and Lei-Han Tang, Phys. Rev. Lett. **64**, 1405 (1990); and the above review papers [2–5].
- [14] M. Lässig, Phys. Rev. Lett. **80**, 2366 (1998).
- [15] M. den Nijs and J. Neergaard, J. Phys. A **30**, 1935 (1997).
- [16] J. Krug, P. Meakin, and T. Halpin-Healy, Phys. Rev. A **45**, 638 (1992).
- [17] M. den Nijs, J. Phys. A **18** (1985) L549-556.
- [18] M. den Nijs, chapter 4 in *The Chemical Physics of Solid Surfaces and Heterogeneous Catalysis*, Vol.7, edited by D. King, Elsevier (Amsterdam, 1994).
- [19] See e.g., H. van Beijeren and I. Nolden, in *Structures and dynamics of Surfaces*, edited by W. Schommers and P. von Blanckenhagen Vol. 2 (Springer, Berlin 1987).

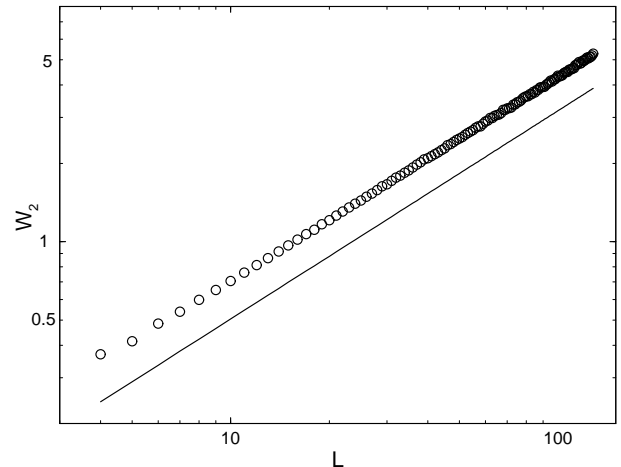


FIG. 1. Stationary state second moment  $W_2$  of the 2D Kim-Kosterlitz (KK) model as function of lattice size  $L^2$ . The solid line with slope 0.8 is shown as reference.

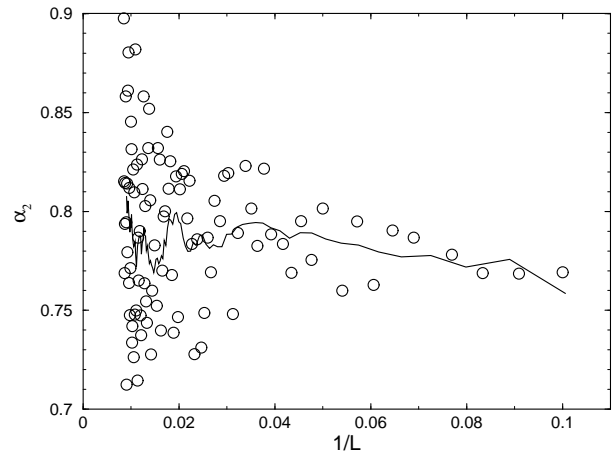


FIG. 2. Finite size scaling approximants for the surface roughness exponent  $\alpha_2$  of the second moment,  $W_2 \simeq AL^{\alpha_2}$ , in the stationary state of the 2D KK model.

- 
- [1] M. Kardar, G. Parisi, and Y-C. Zhang, Phys. Rev. Lett. **56**, 889 (1986).
  - [2] J. Krug and H. Spohn in *Solids Far from Equilibrium: Growth, Morphology and Defects*, ed. C. Godrèche (Cambridge University Press, Cambridge, 1991).
  - [3] P. Meakin, Physics Reports **235**, 189 (1993).
  - [4] J. Krug in *Scale Invariance, Interfaces, and Non-Equilibrium Dynamics*, ed. A. McKane, M. Droz, J. Vanimenuis, and D. Wolf (Plenum, NY, 1995).
  - [5] T.J. Halpin-Healy and Y.C. Zhang, Physics Reports **254**, 215 (1995).
  - [6] M. Lässig and H. Kinzelbach, Phys. Rev. Lett. **78**, 903 (1997); K. Wiese, Phys. Rev. E **56**, 5013 (1997); C. Castellano, M. Marsili, L. Pietronero, Phys. Rev. Lett. **80**, 4830 (1998).
  - [7] D. Dhar, Phase Transitions **9**, 51 (1987).
  - [8] L-H. Gwa and H. Spohn, Phys. Rev. Lett. **68**, 725 (1992); and, Phys. Rev. A **46**, 844 (1992).
  - [9] J. Neergaard and M. den Nijs, Phys. Rev. Lett. **74**, 730 (1995).
  - [10] see e.g., B. Derrida, M.R. Evans, V. Hakim, and V. Pasquier, J. Phys. A **26**, 1493 (1993).
  - [11] J. M. Kim and J. M. Kosterlitz, Phys. Rev. Lett. **62**, 2289 (1989).
  - [12] J.G. Amar and F. Family, Phys. Rev. Lett. **64**, 543 and 2334 (1990); J. Krug and H. Spohn, Phys. Rev. Lett. **64**,

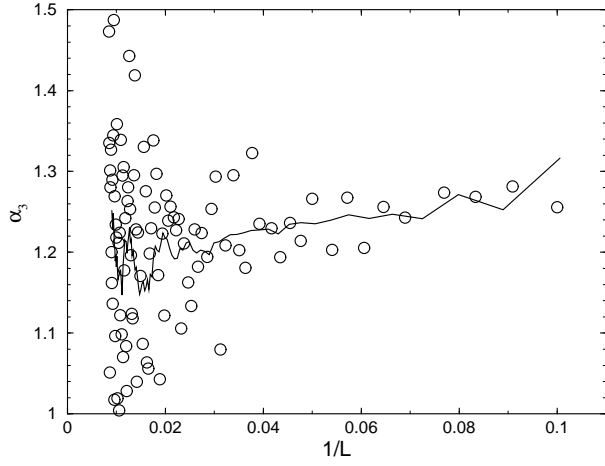


FIG. 3. Finite size scaling approximants  $\alpha_3(L)$  for the surface roughness exponent  $\alpha_3$  of the third moment,  $W_3 \simeq AL^{\alpha_3}$ , in the stationary state of the 2D KK model.

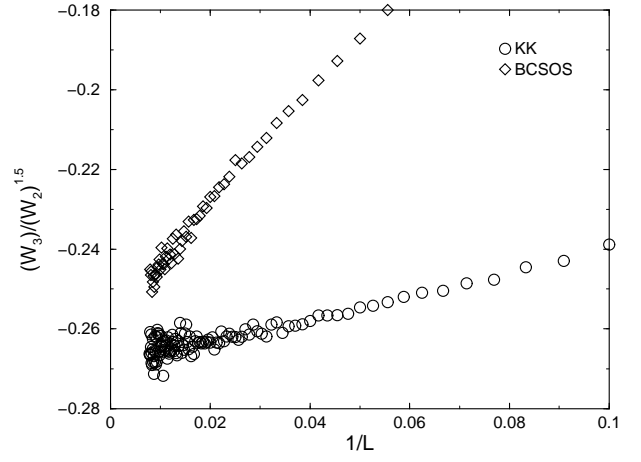


FIG. 5. Finite size scaling behaviour of the skewness amplitude ratio  $R_3 = W_3/W_2^{1.5}$  in the 2D KK model (the circles) and the  $K = 0$  BCSOS model (diamonds).

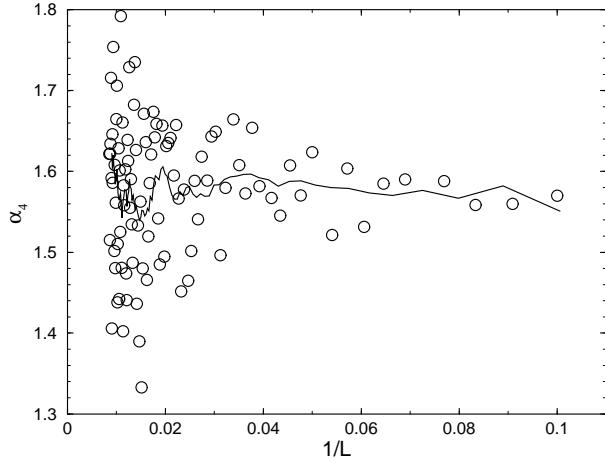


FIG. 4. Finite size scaling approximants  $\alpha_4(L)$  for the surface roughness exponent  $\alpha_4$  of the fourth moment,  $W_4 \simeq AL^{\alpha_4}$ , in the stationary state of the 2D KK model.

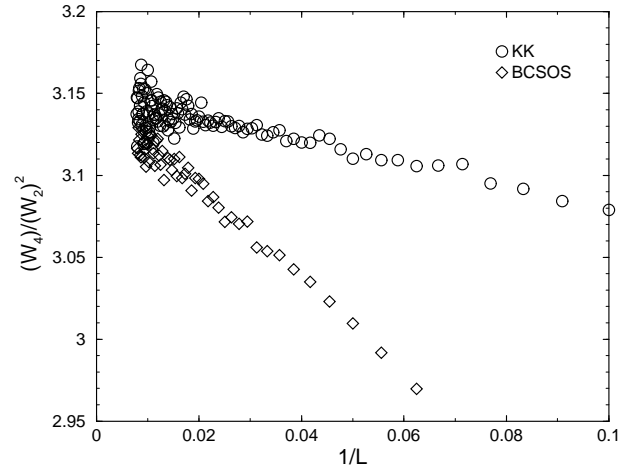


FIG. 6. Finite size scaling behaviour of the fourth moment amplitude ratio  $R_4 = W_4/W_2^2$  in the 2D KK model (the circles) and the  $K = 0$  BCSOS model (diamonds).

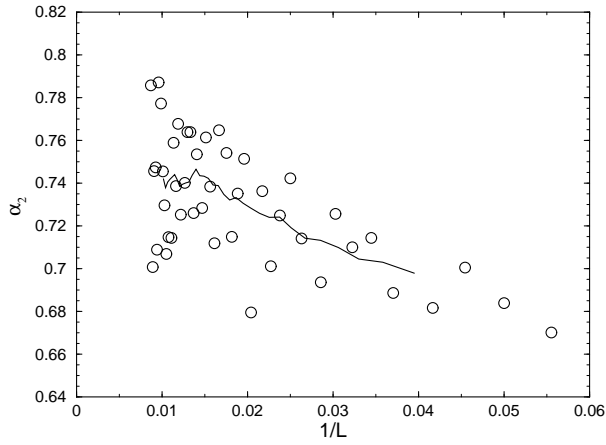


FIG. 7. Finite size scaling approximants for the surface roughness exponent  $\alpha_2$  of the second moment,  $W_2 \simeq AL^{\alpha_2}$ , in the stationary state of the 2D BCSOS model.

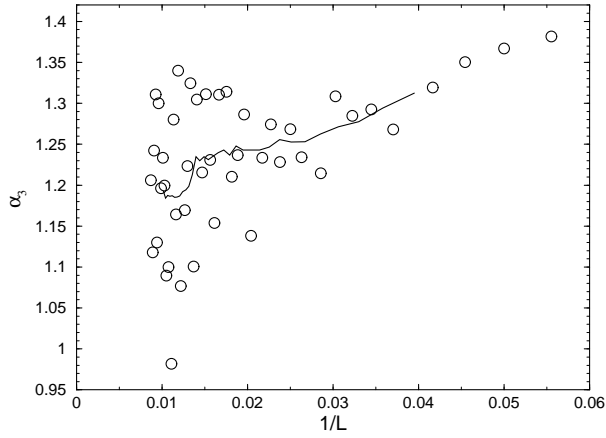


FIG. 8. Finite size scaling approximants for the surface roughness exponent  $\alpha_3$  of the third moment,  $W_3 \simeq AL^{\alpha_3}$ , in the stationary state of the 2D BCSOS model.

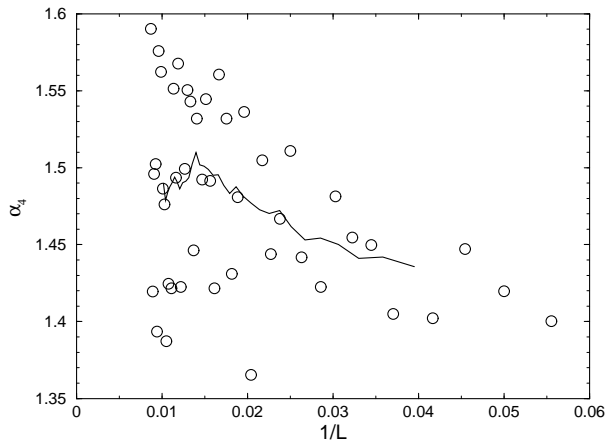


FIG. 9. Finite size scaling approximants for the surface roughness exponent  $\alpha_4$  of the fourth moment,  $W_4 \simeq AL^{\alpha_4}$ , in the stationary state of the 2D BCSOS model.

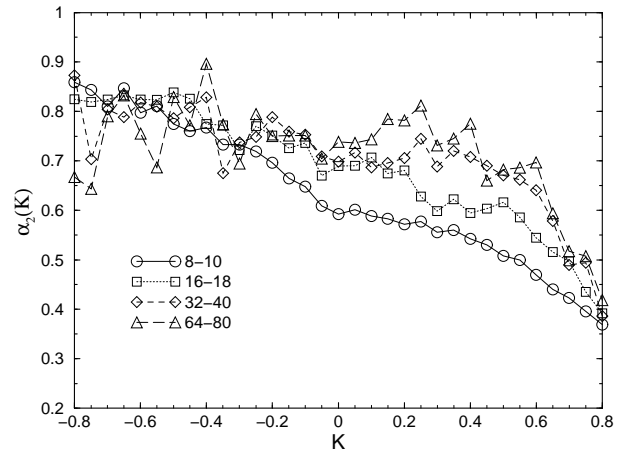


FIG. 10. Finite size scaling approximants for the surface roughness exponent  $\alpha_2$  of the second moment,  $W_2 \simeq AL^{\alpha_2}$ , in the stationary state of the 2D BCSOS model as function of  $K$ .

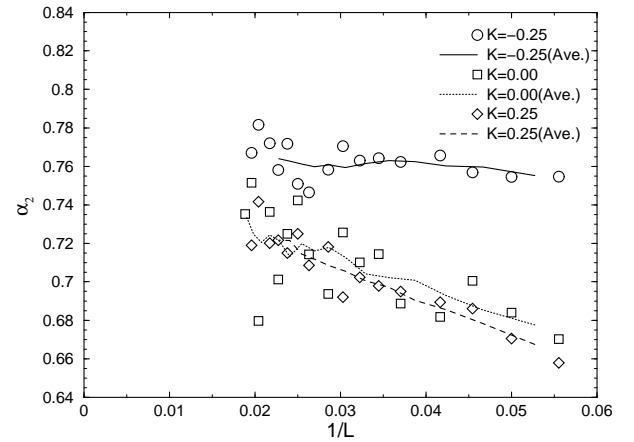


FIG. 11. Finite size scaling approximants for the surface roughness exponent  $\alpha_2$  of the second moment in the stationary state of the 2D BCSOS model at  $K = \pm 0.25$  and 0.



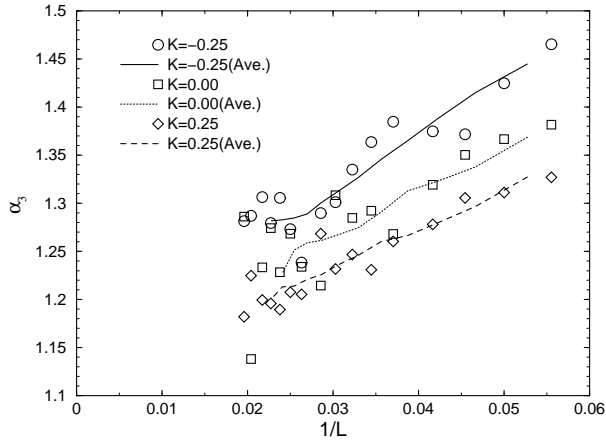


FIG. 12. Finite size scaling approximants for the surface roughness exponent  $\alpha_3$  of the third moment in the stationary state of the 2D BCSOS model at  $K = \pm 0.25$  and 0.

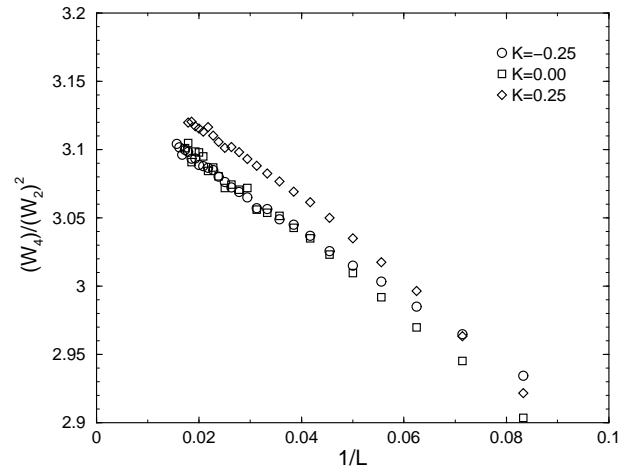


FIG. 15. Finite size scaling behaviour of the fourth moment amplitude ratio  $W_4/W_2^2$  in the stationary state of the 2D BCSOS model at  $K = \pm 0.25$  and 0.

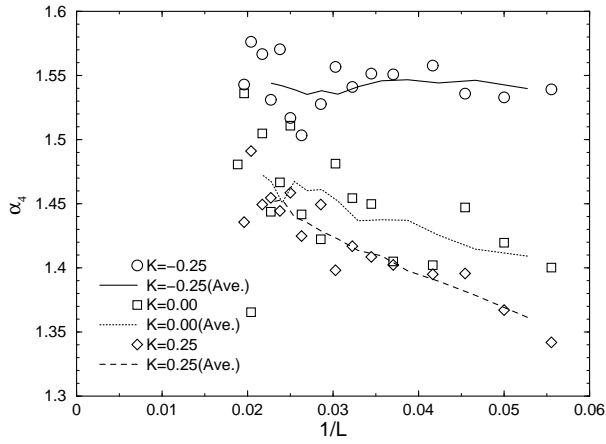


FIG. 13. Finite size scaling approximants for the surface roughness exponent  $\alpha_4$  of the fourth moment in the stationary state of the 2D BCSOS model at  $K = \pm 0.25$  and 0.

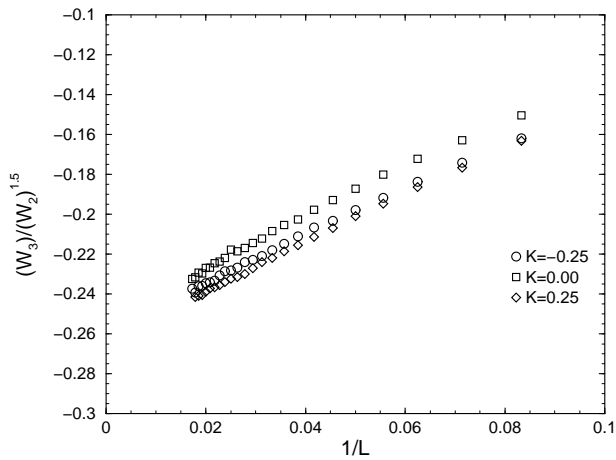


FIG. 14. Finite size scaling behaviour of the skewness amplitude ratio  $R_3 = W_3/W_2^{1.5}$  in the stationary state of the 2D BCSOS model at  $K = \pm 0.25$ , and 0.

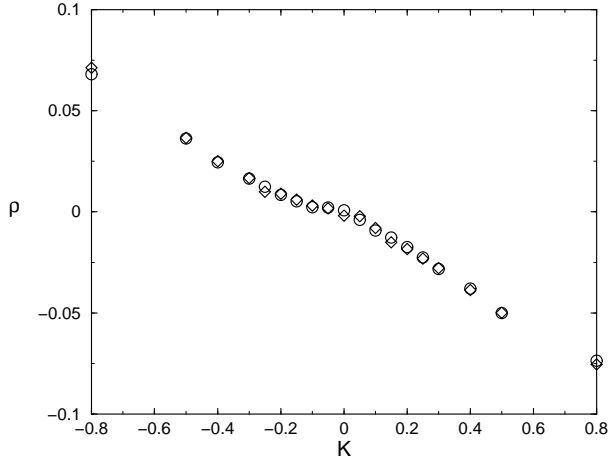


FIG. 16. The difference in the expectation value of local sharp hill tops and of local sharp valley bottoms as function of  $K$  in the 2D BCSOS model along 1D cross sections through the surface. The diamonds (circles) are for lattice size  $L = 36$  (64).

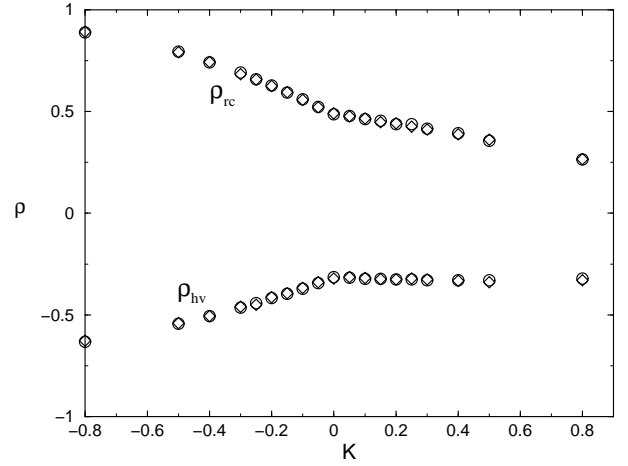


FIG. 17. The difference in the expectation value of sharp hill tops and of sharp valley bottoms,  $\rho_{hv}$ , and local sharp ridges and canyons,  $\rho_{rc}$ , as function of  $K$  in the 2D BCSOS model. The diamonds (circles) are for lattice size  $L = 36$  (64).

hill			valley			ridge			canyon		
h	h+1	h	h+2	h+1	h+2	h+2	h+1	h	h	h+1	h+2
h+1	h+2	h+1	h+1	h	h+1	h+1	h+2	h+1	h+1	h	h+1
h	h+1	h	h+2	h+1	h+2	h	h+1	h+2	h+2	h+1	h
(1)			(2)			(3)			(4)		

FIG. 18. Definition of local sharp hill tops, valley bottoms, ridges, and canyons in the 2D BCSOS model.